BJRS

BRAZILIAN JOURNAL
OF
RADIATION SCIENCES
09-01A (2021) 01-13

Oxide layer characterization by XRD and Rietveld refinements in maraging steel 300 aged in steam atmosphere

Silva[a] V.S.P., Neto[a] J.R.F., Oliveira[a] D.C., Silva[a] S.L.F., Camargo[a] F.

[a] *AMAZUL – Amazônia Azul Tecnologias de Defesa S.A., 05.581-001, São Paulo-SP, Brazil*

vanessa.sanches@marinha.mil.br

ABSTRACT

Maraging steels are martensitic steels hardened by precipitation of intermetallic compounds in thermal aging, with good machining properties and high strength, fracture toughness and corrosion resistance, being used in aircraft parts and rocket motor-case, tooling applications and nuclear plants. During thermal aging in steam atmosphere a protective and corrosion resistant oxide layer is formed over the bulk. In this work, conventional Bragg-Brentano geometry was used to identify the phases formed in four specimens of maraging steel grade 300 with different surface finishes that were previously solution annealed twice at (950 ± 5) °C for 1 h, air-cooled, and submitted to oxidation process under positive pressure about 1.5 kPa of steam at (480 ± 5) °C for 6 h, followed by forced air-cooling. Diffraction patterns were measured employing CuK$_\alpha$ radiation, ranging $20^o < 2\theta < 85^o$ and the Rietveld method was used to better characterize the structures identified. Through Rietveld refinements it was possible to conclude that the layer formed during heat treatment process is constituted by a transition metallic phase with a quasi-cubic face centered unit cell, and an oxide layer that includes hematite, magnetite and a spinel structure type MFe_2O_4, where M could be an alloying element, for all analyzed samples.

Keywords: **Maraging Steel, X-ray Diffraction, Rietveld Method**

ISSN: 2319-0612
Accepted: 2020-11-23

1. INTRODUCTION

Maraging steels offer an unusual combination of high tensile strength, high fracture toughness and high corrosion resistance, in addition to good ductility. The rare combination of these properties found in this kind of steels make them well suited for aircraft parts, aerospace rockets, nuclear plants and others applications that require high strength and damage tolerance [1-3]. The maraging steel is low-carbon martensitic steel with high amount of substitutional alloying element which contains hard precipitate particles formed by thermal aging [3-4]. If this process is made in steam atmosphere, a protective and corrosion resistant oxide layer can be formed over the bulk; this is an advantage of cost and efficiency comparing with other types of coating protection layers [2].

Several characterization methods can be employed to evaluate the oxide layer formed during this process, but many of them involve destructive techniques that are not always convenient to use, and usually focus on the determination of the thickness of the structure in layers typically formed over the bulk, using microscopy techniques (Optical and Scanning Electron Microscopy – SEM) or depth profile techniques (X-ray Photoelectron Spectroscopy – XPS and Glow Discharge Optical Emission Spectroscopy – GDOES) that are able to give composition information about the layers, but no direct information about the crystalline structures formed during the process [2, 5-7].

The profile refinement method proposed by Rietveld in 1967 and 1969 [8-9] compares an entire observed powder diffraction pattern as a whole, with an entire calculated pattern based on a set of refined parameters, such as: lattice parameters, position of the atoms in the unit cell, occupancy, spatial group, profile functions, among other factors, that model the crystal structures possible present in the sample that has been analyzed, using the least-squares method [10]. This is done comparing each i-step intensity observed ($y_i^{(obs)}$) with the i-step intensity calculated ($y_i^{(calc)}$), and adjusting the aforementioned parameters, that are inserted in the chosen model, in order to minimize the following function:

$$S = \sum_i \left[\frac{(y_i^{(obs)} - y_i^{(calc)}}{y_i^{(obs)}} \right] \quad (1)$$

Originally proposed to solve crystal structures using neutron radiation, this method has been extensively used to solve polycrystalline structures based also on X-ray powder diffraction data and synchrotron radiation [11]. In this work, conventional Bragg-Brentano XRD analysis was used to identify the phases formed on specimens of maraging steel grade 300 with different surface finishes and refine these phases through Rietveld method, in order to improve the good-of-fitness (GOF) results and the visual fitting between the experimental and calculated data.

Although Rietveld refinement allows to quantify the phases present in each specimen, as the calculated curve is based on a homogeneous sample with several small crystallites distributed randomly, which does not reflect the case studied here, since it was known that the phases were distributed in layers above the surface [2, 5-6, 12], the quantitative phase analysis was not presented here, because it isn't part of the scope of this work and would require a correction in the software used to perform the fitting procedure [13].

2. MATERIALS AND METHODS

2.1. Specimens preparation

In this work, four samples of maraging steel grade 300 (MA300), were cut to dimensions approximately of 40 × 20 × 5 mm. Then, in a muffle furnace they were solubilized twice at (950 ± 5) °C for 1 h [3-4] and air-cooled, in order to homogenize the alloy matrix.

Before thermal aging, the specimens were mechanically ground by means of silicon carbide abrasive paper from 220 to 1200 grit, then two of them were polished using diamond paste from 6 to 1 μm to obtain a scratch-free surface. Next the samples were submitted to oxidation process under positive pressure around 1.5 kPa of steam at (480 ± 5) °C for 6 h [3-4] followed by forced air-cooling.

The specimens were heat treated in two stacked baskets. In each basket a sanded specimen and a polished one were placed, and because of that, in order to differentiate the samples, the denomination chosen for them is formed by two letters: the first one indicates the position of the basket in which the specimens were treated, on the **t**op (T) or on the **b**ottom (B), and the second one, the surface finish received, **s**anded (S) or **p**olished (P).

2.2. XRD analysis

Diffraction patterns were measured employing CuK_α (λ = 1.5406 Å) radiation in a Bruker diffractometer model D8-Advance, using parallel beam optics, step of 0.02° in step scan mode ranging $20^o < 2\theta < 85^o$.

The phases were first identified using the commercial software Diffrac. EVA from Bruker. At first, this procedure showed the presence of four phases for each specimen: α-iron (ferrite), γ-iron (austenite), Fe_2O_3 (hematite) and Fe_3O_4 (magnetite). These structures were used as first model (cubic version) to calculate the diffraction pattern, through software TOPAS, v. 5, from Bruker, in order to perform the Rietveld refinements.

Due to misfit of the Bragg reflection (2 0 0) on the metallic phases and the knowledge that some maraging steels present tetragonal distortion [14-16], a second model (tetragonal version) was created using equivalent tetragonal structures for these phases.

Finally, looking closely to the magnetite fitting, and knowing it was expected to form possible spinel's structures made not only by iron but also by other alloy elements, a third model (final version) was created by hypothesis, in which an extra structure was inserted to fit the magnetite's reflections.

In the next section a more detailed description about the Rietveld results and the assumptions made during the analysis of the specimens studied in this work will be presented.

3. RESULTS AND DISCUSSION

The phases identified by software Diffrac. EVA, their Inorganic Crystal Structure Database (ICSD) codes, and some relevant information were presented in Table 1.

The calculated diffraction pattern using these phases (first model), by TOPAS software, during Rietveld refinements, was made considering the occupancy of the iron atoms at the metallic phases equivalent to the composition of the MA300 bulk, previously analyzed by X-ray fluorescence (XRF), inserting the majoritarian alloy elements (Ni, Co, Mo, and Ti) in the unit cell considered. After refined the zero point, scale factors and lattice parameters, it was necessary to correct preferential orientation of the crystalline phases, which was done by using preferably the March-Dollase correction, but, in some cases, spherical harmonics.

Table 1: Phases identified for all specimens using Diffrac. EVA software by Bruker.

Phase	Structure unit	Lattice parameter	ICSD code	Related to:
α-iron	bcc	a = 2.866 Å	631724	Martensite bulk
γ-iron	fcc	a = 3.569 Å	185743	Metallic austenite phase formed during aging
Hematite (Fe_2O_3)	hexagonal	a = 5.038 Å c = 13.772 Å	15840	Oxide phase formed during aging
Magnetite (Fe_3O_4)	cubic	a = 8.397 Å	75627	Oxide phase formed during aging

The metallic phases had three Bragg reflections in the range analyzed, and by using the cubic model, even after performed the corrections described above, complemented by roughness and tilt corrections, the peaks in the middle angles, (2 0 0) for both phases, were slightly dislocated, although the other reflections presented good fittings.

Because of that, as told before, the cubic structures were replaced by equivalent tetragonal structures. The decision to consider the γ-phase, hereby called austenitic phase, tetragonally distorted was taken not only because of the experimental evidence of (2 0 0) reflection misfitting, but also because the literature indicates that this phase is formed due to migration of iron from bulk to the layer of oxides, which generates this intermediate layer depleted in iron that stabilizes the more compact fcc structure [2, 12], and as it seemed that the bulk, from where it originates, had this tetragonal distortion, it was hypothesized that this distortion would also affect this phase formed between the matrix and the oxide layer.

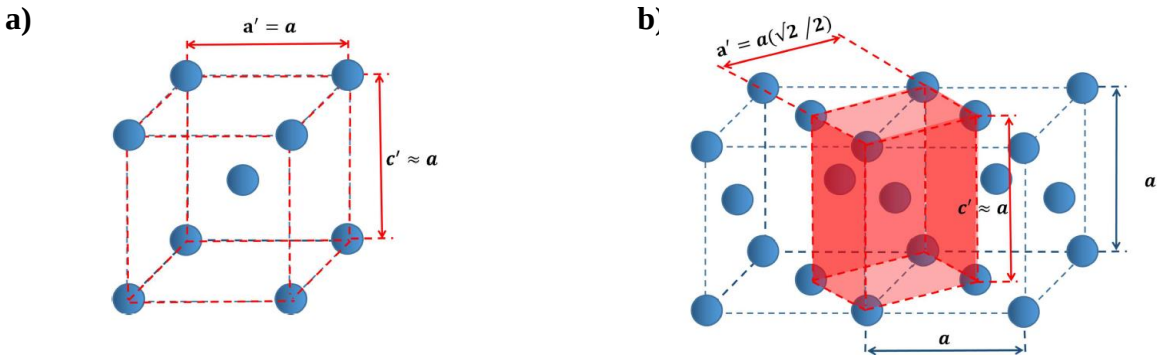

Figure 1: *Relationship between the lattice parameters under the transformation of a) a cubic body centered cell to a tetragonal one; b) a cubic face centered cell to a tetragonal body centered cell.*

The tetragonal body centered martensite phase was refined from a tetragonal structure, I4/mmm space group, with $c \approx a = (2.87 \pm 0.05)$ Å, where the lattice parameter value was based on the mean value previously found in the cubic model after Rietveld refinement. Since a slightly tetragonal face centered structure ($a; b = a; c \approx a$) is equivalent to a tetragonal body centered one with $a' = \left(\sqrt{2}/2\right)a; b' = a'$ and $c' = c \approx a$, see Figure 1, the mean lattice parameter encountered in previous model for fcc phase ($a = 3.57$ Å) was used to create the slightly tetragonal austenitic phase, using I4 /mmm space group, with $a' = (2.52 \pm 0.05)$ Å and $c' = (3.57 \pm 0.05)$ Å.

Figure 2 presents in detail the improvement of the (2 0 0) cubic peak fitting when the second model (right plots) was used instead of the first one (left plots). These visual fittings improvement can be directly associated with the decrease of the GOF parameters of each analysis presented in Table 2.

Table 2: GOF from Rietveld method applied to the four specimens using different models for calculated powder diffraction pattern.

Specimens	**Cubic Version (1st model)**	**Tetragonal Version (2nd model)**	**Final Version (3rd model)**
TP	1.27	1.10	1.08
TS	1.09	1.05	1.05
BP	1.65	1.13	1.06
BS	1.15	1.08	1.05

The GOF value, presented in Table 2, is related to the most knowing "chi squared" (χ^2) value as $GOF^2 = \chi^2$. Briefly, it indicates how close the weighted profile R-factor value (R_{wp}) is to the expected R-factor (R_{exp}), and the closer GOF value is to unit the better is the adjustment of the theoretical model to the measured diffraction pattern [17]. It was chosen to evaluate how good was the Rietveld analysis performed and to compare the improvement obtained by using the different models analyzed here.

Although the GOF values of the second model were already acceptable, knowing that the low value obtained was strongly influenced by the high background measured during the XRD, and that other spinel structures could be formed during aging, besides to desire the improvement of magnetite's peak fitting, a third model (final version) was created with a fifth structure to fitting the magnetite's reflections.

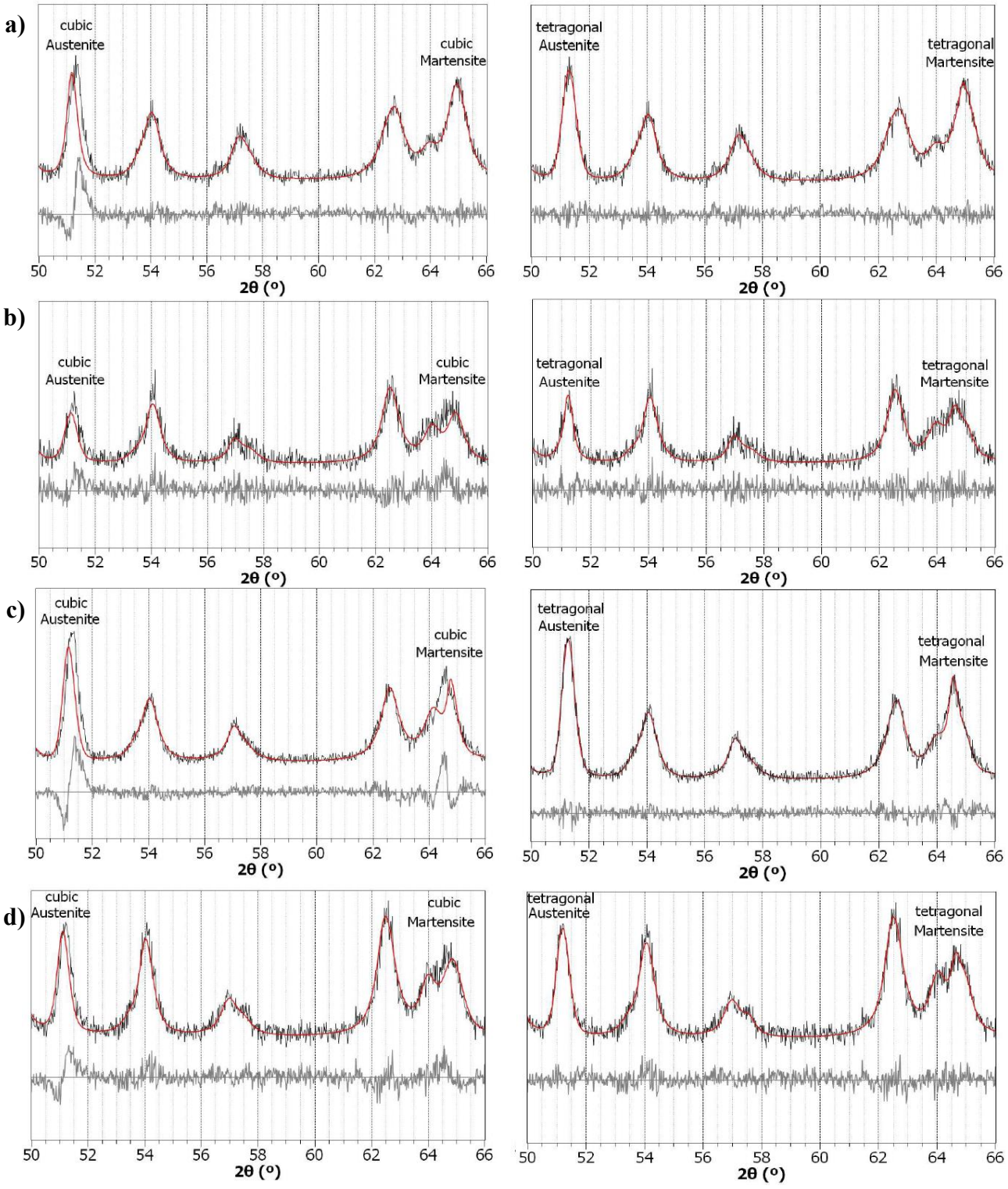

Figure 2: *Fitting detail of a) TP, b) TS, c) BP and d) BS patterns using cubic (first model on the left) and slightly tetragonal (second model on the right) structures for the metallic phases.*

Best results were found when a trigonal spinel, R-3mH space group was used, in conjunction with the magnetite cubic phase, in this final model.

Figure 3 shows the diffraction patterns observed from the Bragg-Brentano XRD analysis (black line), the calculated patterns (red line) from the Rietveld method using the final version of the models tested and the difference curve (gray line). Observing the diffractograms and comparing the visual fitting of the diffraction patterns calculated to those observed, we conclude that the proposed model has a high correlation with the analyzed samples, and no reflection was left out of the third model. The simplest way to evaluate that is paying attention to the difference curve, if it stays around the zero value, i.e. the straighter the dark gray line, the better the Rietveld results.

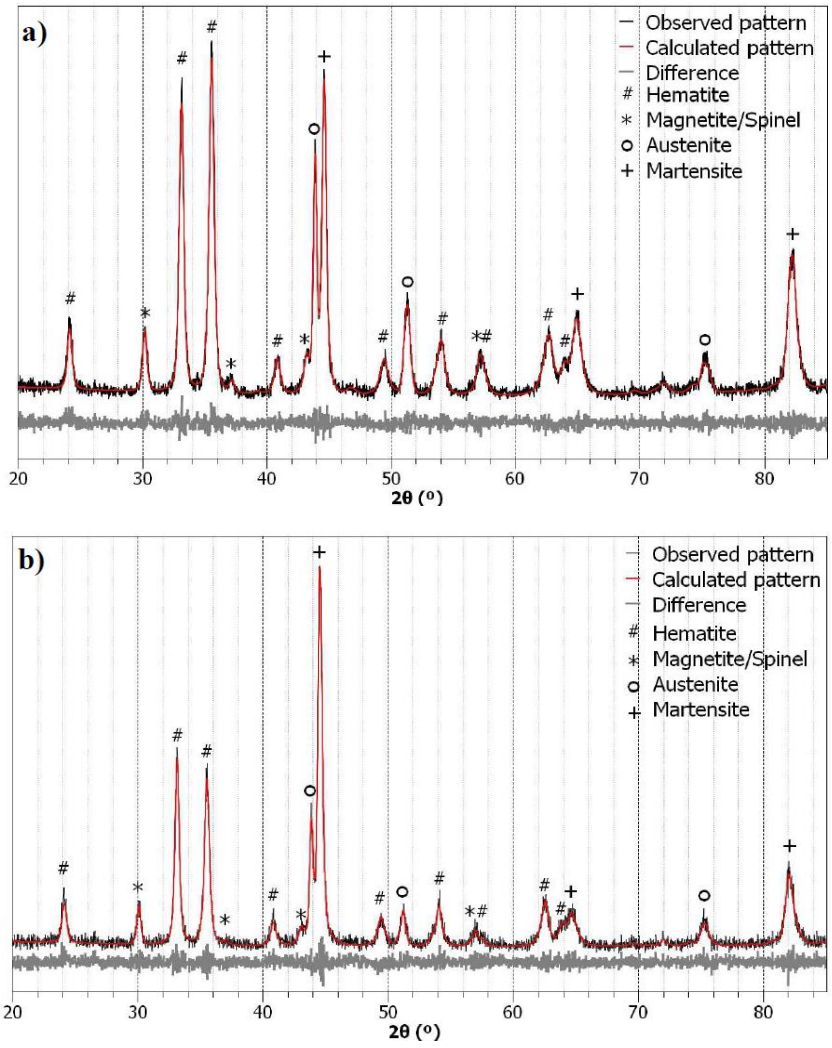

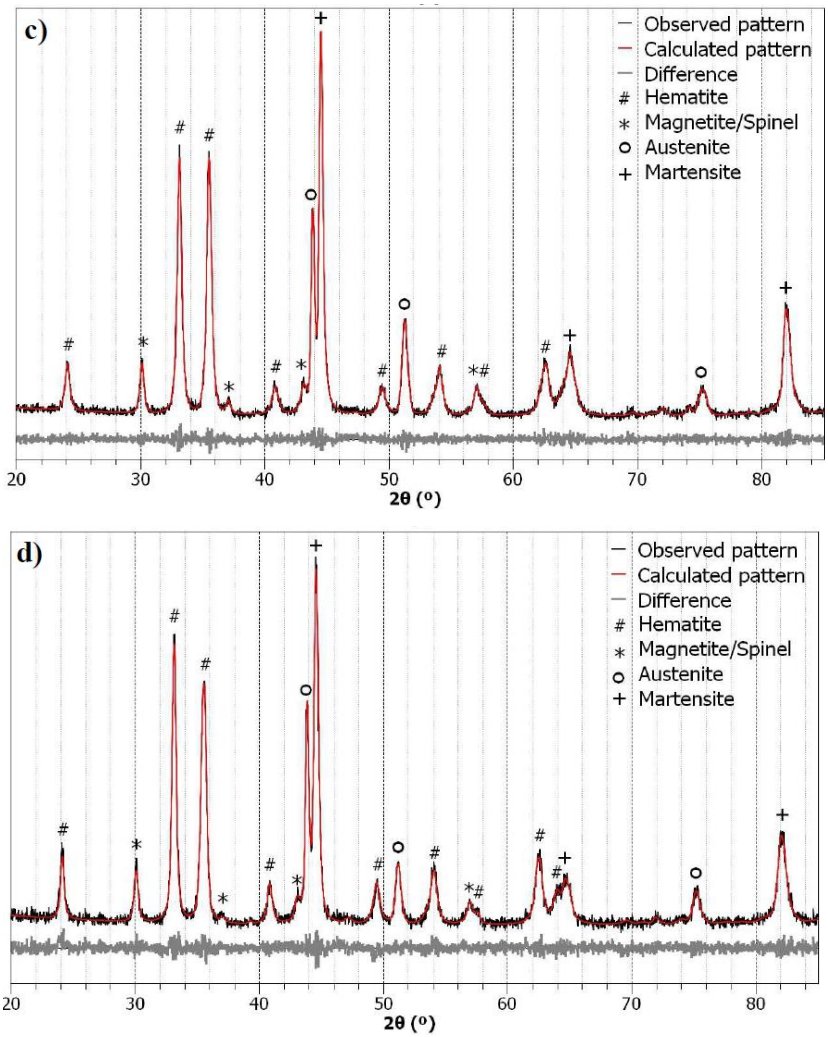

Figure 3: *Observed, calculated and difference CuK$_\alpha$ powder diffraction patterns for a) TP, b) TS, c) BP and d) BS specimens by using final version modelling*

Results of the lattice parameters refined using the third model are shown in Table 3. In the austenite phase, the a' and c' values are the output values from the software and the a-value refers to the calculated of the a equivalent tetragonal face centered cell value, as explained before. The "diff (%)" column indicates the tetragonal distortion of the cubic cell, e.g., the percentage difference between a and c parameters (or c' for austenite phase).

It is possible to notice that the unit cells that presented the greatest distortion, for example, the polished specimens for the austenitic phase are those that presented the worst fit of the calculated curves to the diffraction pattern measured when the cubic model was used (Figures 2a and 2c). On

the other hand, the TP specimen, that presents the smallest distortion on the martensite lattice parameter, according to Table 3, was the one on which the change to a tetragonal body centered phase almost did not affect the calculated peaks position (Figure 2a).

Table 3: Lattice parameters of the final version used in the Rietveld method for the metallic phases, showing their slightly tetragonal distortion.

	Austenite phase				**Martensite phase**		
Specimens	a' **(Å)**	a **(Å)**	c' **(Å)**	**diff (%)**	a **(Å)**	c **(Å)**	**diff (%)**
TP	2.515	3.590	3.557	0.93%	2.874	2.862	0.41%
TS	2.520	3.584	3.564	0.55%	2.882	2.864	0.63%
BP	2.517	3.589	3.560	0.81%	2.883	2.865	0.64%
BS	2.523	3.586	3.568	0.50%	2.881	2.866	0.52%

The same kind of observation can be done about the other specimens, and all of them show the consistency of the model chosen for refining both metal phases, the martensitic matrix and the almost cubic face centered phase, that is being called austenite, and was formed during the oxidation process for all specimens under study. Unfortunately, no significant conclusions could be drawn regarding the influence of the surface finish of the specimens.

Moreover, as Nunes and et. al. [15] showed that, in the temperature studied here (480 °C), the austenite reversion during aging was not observed and since the signal from the martensite matrix of MA300 appears in all diffractograms collected, the phases formed during the oxidation process must be in a layer which is thin enough to allow the penetration of the X-rays reaching the bulk, but thick enough to present reflections greater than the high background obtained mainly due to iron fluorescence, which is in accordance with the typical layered structure formed during aging in steam [2, 5-6, 12].

4. CONCLUSION

In this work the analysis of the specimens treated under positive pressure around 1.5 kPa of steam at (480 ± 5) °C for 6 h followed by forced air-cooling, showed the formation of a quasi-cubic

face centered cell phase, called austenite here, and an oxide mixture composed by hematite, magnetite and a spinel structure formed probably by the oxidation of some alloying elements.

It was not possible to verify any conclusive influence of the superficial prior finishing received by the samples, but the Rietveld methodology was shown to be important in the characterization of the phases formed in this process, since besides the refining of the lattice parameters has revealed the distortion in the unit cell on the metallic phases it also presented evidence of the presence of another phase not previously identified by typical search & match procedure done by Diffrac. EVA software.

Therefore, the main conclusion that can be drawn from the results is that all the specimens of MA300 treated in this work have a martensitic matrix of body centered tetragonal crystalline structure, and not cubic, and that during the oxidation process the intermediate layer formed, through the migration of the iron to the oxide layer, is also tetragonal, but equivalent to a quasi-cubic face centered structure, having a slight distortion, less than 1 %, on one of its lattice parameters.

It is important to point out that, due to the fluorescence of the iron, the diffraction pattern data had high background and low counting statistics, so a future work using cobalt X-ray tube would be extremely important to corroborate the conclusions listed here. Besides, a better understanding of the spinel phase, especially its composition, could be made by using synchrotron light source with wavelengths at the absorption edge of the iron or cobalt, because in this case not only the data collection could be done with an appropriate statistic to the Rietveld's analysis, but the occupancy factors could also be reliably refined.

ACKNOWLEDGMENT

The authors are grateful for the support and encouragement received from their Institution, especially from Ana Elis Lopes Claudio, who motivated us along this work, knowing its particular importance for the formation of her work team and Odair Doná Rigo for the results discussion, knowledge transferred and incentive.

REFERENCES

[1] TEWARI R.; MAZUMDER S.; BATRA I.; DEY G.; BANERJEE S. Precipitation in 18 wt% Ni maraging steel of grade 350. **Acta Materialia**, v. 48, p. 1187-1200, 2000.

[2] REZEK J.; KLEIN I. E.; YAHALOM J. Structure and corrosion resistance of oxides grown on maraging steel in steam at elevated temperatures. **Applied Surface Science**, v. 108, p. 159-165, 1997.

[3] SHA W.; GUO Z. **Maraging Steels: Modelling of Microstructure, Properties and Applications**, 1st ed., New York: Woodhead Publishing Limited, 2009.

[4] MAGNEE A.; DRAPIER J. M.; COUTSOURADIS D.; HABRAKAN L.; DUMONT J. Cobalt-containing high-strength steels. **Centre D'information Du Cobalt**, Brussels, 1974.

[5] QUADAKKERS W. J.; ENNIS P. J.; ZUREK J.; MICHALIK M. Steam oxidation of ferritic steels - laboratory test kinetic data. **Materials at High Temperatures**, v. 22, p. 47-60, 2005.

[6] ENNIS P. J.; QUADAKKERS W. J. Mechanisms of steam oxidation in high strength martensitic steels. **International Journal of Pressure Vessels and Piping**, v. 84, p. 75-81, 2007.

[7] SUZUKI S.; KAKITA K. A Comparative Study of GDOES, SIMS and XPS Depth Profiling of Thin Layers on Metallic Materials. **Journal of Surface Analysis**, v. 12, p. 174-177, 2005.

[8] RIETVELD H. M. Line profiles of neutron powder-diffraction peaks for structure refinement. **Acta Crystallographica**, v. 22, p. 151-152, 1967.

[9] RIETVELD H. M. A profile refinement method for nuclear and magnetic structures. **Journal of Applied Crystallography**, v. 2, p. 65-71, 1969.

[10] CPD - Commission on Powder Diffraction; IUCr - International Union of Crystallography. **Rietveld Refinament from Powder Diffractin Data**, n. 26, 2001.

[11] WILL G. **Powder Diffraction: The Rietveld Method and Two-Stage Method**, 1st ed., Berlin: Springer, 2006.

[12] KLEIN, I. E.; YANIV, A. E.; SHARON, J. The Oxidation Mechanism of Fe-Ni-Co Alloys. **Oxidation of Metals**, v. 16, p. 99-106, 1981.

[13] TAGLIENT, M. A.; PENZA M.; GUSSO M.; QUIRINI A. Characterisation of ZnS:Mn thin films by Rietveld refinement of Bragg-Brentano X-ray diffraction patterns. **Thin Solid Films**, v. 353, p. 129-136, 1999.

[14] NUNES G. C. S.; SARVEZUK P. W. C.; BIONDO V.; BLANCO M. C.; NUNES M. V. S. Structural and magnetic characterization of martensitic Maraging-350. **Journal of Alloys and Compounds**, v. 646, p. 321-325, 2015.

[15] NUNES G. C. S.; SARVEZUK P. W. C.; ALVES T. J. B.; BIONDO V.; IVASHITA F.; PAESANO JR. A. Maraging-350 steel: Following the aging through diffractometric, magnetic and hyperfine analysis. **Journal of Magnetism and Magnetic Materials**, v. 421, p. 457-461, 2017.

[16] ALVES T. J. B.; NUNES G. C. S.; TUPAN L. F. S.; SARVEZUK P. W. C.; IVASHITA F. F.; OLIVEIRA C. A. S.; PAESANO JR. A. Aging-Induced Transformations of maraging-400 Alloys. **Metallurgical and Materials Transactions A**, v. 49, p. 3441–3449, 2018.

[17] TOBY B. H. R factors in Rietveld analysis: How good is good enough? **Powder Diffraction**, v. 21, p. 67-70, 2006.